Sub-Å Resolution Electron Density Analysis of the Surface of Organic Rubrene Crystals

Yusuke Wakabayashi,[1,*] Jun Takeya,[2] and Tsuyoshi Kimura[1]

[1]*Division of Materials Physics, Graduate School of Engineering Science, Osaka University, Toyonaka 560-8531, Japan*

[2]*Graduate School of Science, Osaka University, Toyonaka 560-0043, Japan*

(Received 17 November 2009; published 12 February 2010)

The electron density distribution of an organic semiconductor is observed as a function of the depth from the crystal surface or interface. The surface x-ray scattering technique combined with a recently developed analyzing technique, coherent Bragg rod analysis, enables us to observe the electron density profile. The obtained near-surface electron density profile of a single crystal of rubrene, which is known as a high-mobility organic transistor material, shows not only a large positional distribution of the molecules at the surface, but also a sub-Å molecular deformation that affects the molecular orbital.

DOI: 10.1103/PhysRevLett.104.066103 PACS numbers: 68.35.bm, 68.35.bg, 73.61.Ph

Organic materials show various electronic properties, and their interface doubles the significance. For example, an interface between two insulating molecular crystals shows metallic conductivity [1], an interface between a magnetic electrode and an organic crystal makes a spintronic system [2], and an interface between a gate insulator and an organic material forms a field effect transistor [3]. The physical property of organic materials is known to have a strong correlation with their structures, and the molecular orbital calculation based on the structures provides a good explanation of their electronic properties [4]. X-ray structure analysis is therefore widely used to provide the structural data, which make it possible to perform a theoretical calculation. When we focus on the interfacial properties, the structural information at the interface is desired. However, near-surface or interface structure of an organic material down to several-nanometer depth with sub-Å resolution has not been reported. In this Letter, we present the first observation of the electron density of an organic transistor material rubrene ($C_{42}H_{28}$) as a function of the depth. The result shows that the surface structural relaxation does alter the energy of the molecular orbitals.

Rubrene is known as a high-mobility organic transistor material. Both amorphous and single crystals of this material work as field effect transistors (FET), and the mobility of the latter is larger than amorphous silicon [5,6]. The structures of the rubrene molecule and crystal are shown in Fig. 1(a) [7]. A rubrene molecule consists of a nearly flat tetracene backbone with four phenyl groups. The symmetry of the crystal is orthorhombic *Bbam*, and the lattice parameters are known as $a = 7.18$ Å, $b = 14.43$ Å, and $c = 26.90$ Å. The surfaces of as-grown samples are parallel to the c-plane, and the molecules form layers having the thickness of $c/2$. Until now, the surface structure of the rubrene single crystal has been studied by atomic force microscopy (AFM) [8] and scanning tunneling microscopy (STM) [9] techniques. Molecular images at the surface obtained by these methods have Å resolution and contain no information in the depth direction.

The depth dependence of the structure of traditional semiconductors, metals, and metal oxides has been studied by surface x-ray scattering method [10,11]. Sudden termination of a crystal gives rise to a rod-shaped scattering perpendicular to the surface, which is called crystal truncation rod (CTR) scattering. The amplitude of this rod-shaped scattering is proportional to the Fourier transformation of the electron density distribution around the surface, and therefore one can study the near-surface structure from the CTR intensity profile.

Plate-shaped single crystals were made by the physical vapor transport method. The typical size of the sample was 3 mm × 3 mm with several micrometers of thickness, and the AFM image (not shown) indicated that the as-grown crystals have step surfaces parallel to the c-plane with the size of the terrace larger than several micrometers and the step height of $c/2$. The crystals were placed on Si (001) substrates whose surfaces were covered with 500 nm-thick SiO_2 insulating layers. The surface x-ray scattering experiment was carried out at BL-4C of the Photon Factory, KEK, Japan. The beam line is equipped with a standard four-circle diffractometer having a scintillation counter. All the experiments were made in air at room temperature, and the data were collected by transverse scans to subtract the background properly.

Figure 1(b) shows the scattered x-ray intensity distribution along the 00ζ direction for a rubrene single crystal. Bragg reflections were observed at $\zeta = 2n$ (n: integer) positions, and clear CTR intensity was observed up to $\zeta = 14.4$ except for a limited region around $\zeta = 9$. The small sample size prevents performing a quantitative measurement below the $\zeta < 4$ region, where the incidence angle was too shallow. Although we measured up to $\zeta = 19$, no CTR intensity was observed above $\zeta = 14.4$ due to the poor statistics. In the present experimental condition, we have not seen a remarkable x-ray radiation effect on the scattered x-ray profile.

The CTR scattering was caused by both sides of the rubrene surfaces, i.e., the interface between the rubrene and air as well as that between the rubrene and the sub-

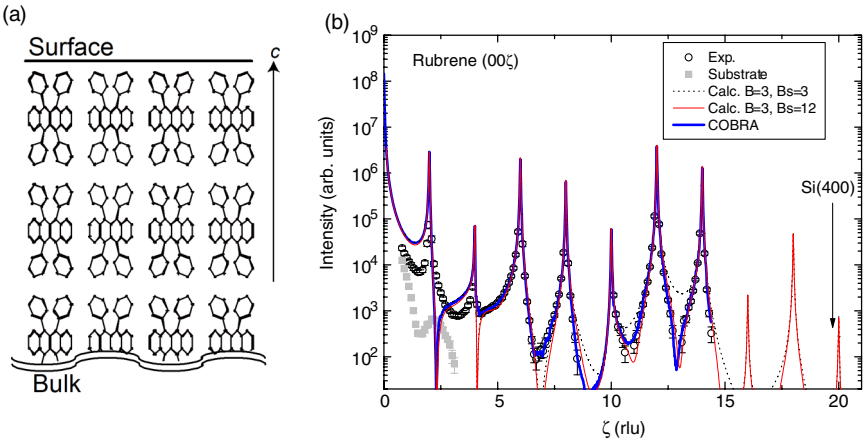

FIG. 1 (color online). (a) The structure of rubrene single crystal [7]. (b) The CTR profile along the 00ζ rod. Gray squares show the CTR profile from the substrate, and open circles show the CTR profile from the rubrene. The dashed curve shows the simulated curve with $B = B_S = 3.0$, the (red) thin solid curve shows that with $B_S = 12.0$, and the (blue) thick curve shows the result of the COBRA (see text).

strate. However, as described below, no information about the substrate will appear in the result of our analysis because of the ζ region used for our analysis. We analyzed the CTR intensity within the $4 < \zeta < 14.4$ region of rubrene on account of the limitation placed by the sample size and the signal intensity as mentioned above. On the other hand, the CTR intensity from the substrate was intense enough to observe only below $\zeta \sim 3$ as shown in Fig. 1(b) with gray squares; the first Bragg reflection from the substrate along this line appears around $\zeta = 19.8$, and thus $\zeta = 14.4$ is far enough from 19.8 to expect any observable CTR amplitude from the substrate. Therefore, the data we analyzed do not contain noticeable amounts of scattering amplitude from the substrate.

The dashed line in Fig. 1(b) shows the calculated profile for the ideal surface model, which has no reconstruction, relaxation, or surface roughness. In this structural model, all the atoms have the isotropic displacement parameter B of 3.0, which is a common value for molecular crystals at room temperature. A better fit to the experimental result, shown by the red solid curve in the same figure, was obtained by assuming 4 times larger displacement parameter for the atoms in molecules only at the surface ($B_S = 12$) than $B = 3.0$ for other atoms inside the crystal. The excellent agreement with the experimental value shows that the surface structure is well reproduced by this structural model, and that both sides of the surfaces have the same structure. However, there is some ambiguity such as the decay depth for the surface effect on B and molecular deformation. Although those values can be, in principle, taken into account for the model calculation, the number of the parameter is too large to make ordinary least-squares fitting. Even if we neglect hydrogen atoms, we still have 42 carbons in a molecule. This means 82 parameters (the atomic position along the c axis and the displacement parameter, z and B, respectively) for one molecule, and if we take three molecular layers into account for fitting, we need to treat 246 parameters.

Instead of making a least-squares fitting, we adopt the coherent Bragg rod analysis (COBRA) [12–15] to obtain a depth profile of the electron density. Since an electron density analysis requires a wide q range of intensity data, we substituted the experimental data with calculated intensity below $\zeta = 4.0$ and some regions having almost no intensity. This substitution is valid because the intensity distribution below $\zeta = 4.0$ is not very sensitive to the structural surface relaxation or adhesive atoms.

The COBRA gives the CTR profile shown by the thick solid curve in Fig. 1(b). The resulting electron density is presented in Fig. 2. The negative z region corresponds to outside the rubrene crystal, and the positive z region corresponds to inside the crystal. Flat and very low electron density in the outside region ensures the phase given by the

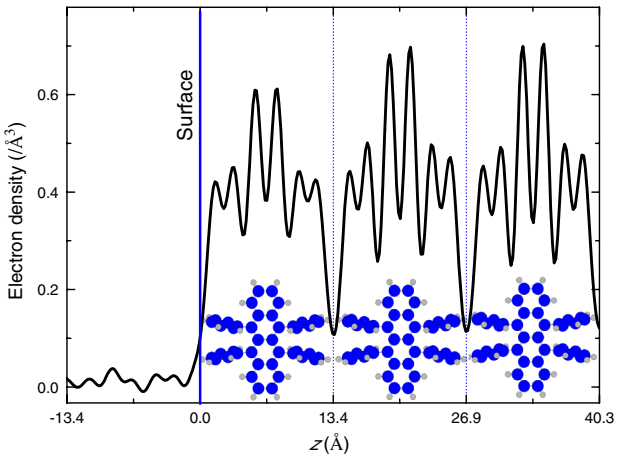

FIG. 2 (color online). The depth dependence of the electron density $\rho(z)$. A schematic view of the rubrene molecules is also shown to present the position and the size of the molecules.

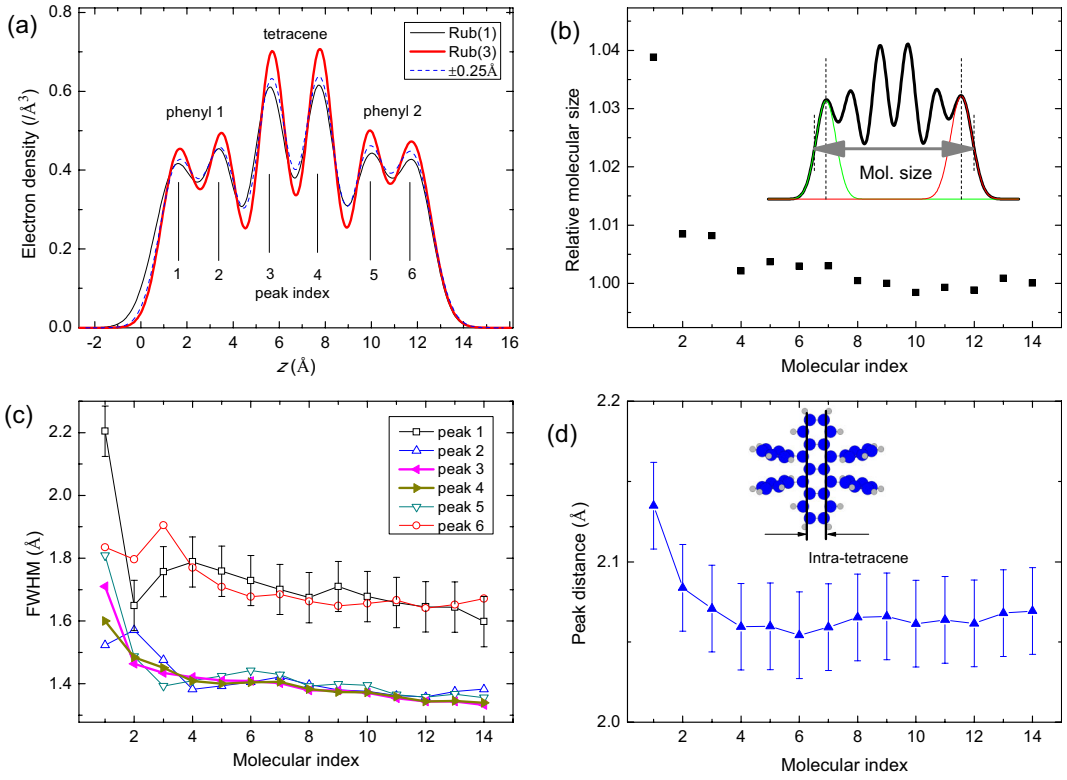

FIG. 3 (color online). (a) The electron density profile for the molecule at the first layer, Rub(1), and the third layer, Rub(3) extracted from Fig. 2 by multi-Gaussian fitting. The profile for $[\rho(z - 0.25\ \text{Å}) + \rho(z + 0.25\ \text{Å})]/2$ for Rub(3) is also shown. (b) Molecular size defined by the sum of the peak distance between peaks 1 and 6 and the values of the half width at half maximum for them as a function of the depth. (c) Peak widths of the six peaks as functions of the depth. (d) Depth dependence of the intratetracene peak distance.

COBRA is correct. It also shows there are a small number of adhesive molecules on the surface (less than 0.02 electrons/Å^3). Because of the symmetry of the material, all the molecules in one layer are superimposed when we project the electron density to the z axis, and molecules belonging to the different layer are well separated. A schematic view of the molecules is placed in this figure to show the size and the position of molecules. There are six peaks in $\rho(z)$ within the size of a molecule. Each pair of phenyl groups, tetracene backbone, and the other pair of phenyl groups gives two peaks. In order to separate the molecules from their neighbors, the electron density for each molecule was fitted to six Gaussians. Figure 3(a) shows the electron density profile of the rubrene molecules at the first layer and at the third layer. We call the molecule at mth layer Rub(m), and m will be called the molecular index. The left-hand side of this figure is closer to the surface, and the profiles are aligned by the right-hand side of the molecule.

Before examining the electron density in detail, we inspected the quality of the result of this analysis. The only values we can know *a priori* are the electron numbers for the pair of phenyl groups and the tetracene backbone, 82 and 116. The integrated electron numbers for them down to 14 layers fall within 83.5 ± 2 and 112.5 ± 1, respectively. The accuracy of these values estimated from the result of the same analysis made on the error-free simulated CTR profile along 00ζ up to $\zeta = 14.5$ are ± 2 and ± 4. The flat depth dependence and the correct electron number ensure the reliability of our analysis.

Comparing the electron density $\rho(z)$ of Rub(1) and Rub(3) shown in Fig. 3(a), one can find two distinct features. One is that the size of Rub(1) is apparently larger than that of Rub(3). The depth dependence of the molecular size, which is defined by the sum of the distance between peaks 1 and 6 and the values of the half width at half maximum for them, is shown in Fig. 3(b). Molecules belonging to the first layer are significantly larger than others, and this deformation is limited to a very shallow region, one or, if any, two layers. The amount of the molecular expansion is 0.4 Å. The other difference is the contrast of $\rho(z)$. Since the peak area is constant, this change in contrast indicates the different positional distribution of the atoms in Rub(1). The dashed curve in panel (a) shows the $[\rho(z - 0.25\ \text{Å}) + \rho(z + 0.25\ \text{Å})]/2$ for Rub(3). This curve reproduces the contrast of the ρ for Rub(1), indicating that the molecular displacement at the first layer is about 0.5 Å. Note that the size of the molecule is not changed significantly by this process, showing that both the molecular expansion and larger z- (height) distribution occur in the first layer.

The depth dependence of the height distribution of the molecules, which is represented by B parameters, was estimated from the peak widths of the electron density

profile. The widths of the six peaks for each molecule are shown in Fig. 3(c). Here, the peak indices 1 and 2 represent the surface-side phenyl groups, 3 and 4 represent the tetracene, and 5 and 6 represent the bulk-side phenyl groups, respectively, [see panel (a)]. Peaks 1 and 6 are broader than the others, meaning that the positions of the carbon atoms for these peaks are widely distributed in the bulk structure. Significant broadening was observed for the peak 1 of Rub(1), the outermost peak. The magnitude of the whole molecular height distribution was estimated by the widths of peaks 3 and 4, the peaks for the tetracene. Larger z distribution is observed at the surface, and the distribution gets smaller within a few layers. These features indicate that no significant surface reconstruction, such as a large tilting of the molecules, happens at the surface of rubrene. The reconstruction is less than 0.5 Å of molecular displacement in the z direction, and the structural relaxation is limited to a couple of layers. This shallow relaxation depth is caused by the weak interlayer van der Waals interaction.

Last, the molecular deformation is examined through the distances between the peaks. The peak distances are classified into three species, intraphenyl (1–2 and 5–6), phenyltetracene (2–3 and 4–5), and intratetracene (3–4) peak distances. Among them, the intratetracene peak distance is the most important because the highest occupied molecular orbital (HOMO) of rubrene is on the tetracene backbone [16], and therefore the deformation of the tetracene backbone directly affects the HOMO state. The intratetracene peak distance presented in panel (d) shows an increase by 0.1 Å around the surface. If we assume that this increase is a static expansion of C-C bonds at the midpoint of peaks 3 and 4, the decrease of HOMO energy by 0.1 eV is derived based on our LDA molecular orbital calculation [17]. Note that although the intratetracene peak distance closely relates to the C-C bond lengths, they are not identical. The reason is that each of the peak 3 and peak 4 is given by the sum of the electron densities of nine carbon atoms, in which only five form the relevant C-C bonds, and four hydrogen atoms. More precise structural information will be given by making similar measurements under a low temperature, which decreases the thermal fluctuation.

The decrease in HOMO energy disturbs hole accumulation at the outermost layer. The holes in rubrene FET may accumulate at the second layer where little lattice relaxation is found. This relaxed surface can be used as a monolayer-thick insulating layer under low-temperatures, if we find an electrode material that suppresses the surface relaxation of the rubrene crystal. The surface relaxation of the organic material was found to affect the molecular orbital considerably, and the sub-Å resolution depth profile is highly important for studying the properties of surface or interface of organic system.

To summarize, we have carried out a coherent Bragg rod analysis on the result of the surface x-ray scattering profile from an organic system, and successfully obtained the electron density profile of the organic transistor material rubrene as a function of depth for the first time. This success indicates the possibility of the microscopic study of organic interfaces and devices, which helps to design new molecules to improve device performance. Similar measurements on FET devices are in progress.

The authors thank Dr. J. P. Hill and Dr. S. B. Wilkins for valuable discussion, and Mr. T. Honda and Professor K. Kusakabe for the help for performing the molecular orbital calculation. This work was supported by KAKENHI (21740274) and Global COE Program (G10).

*wakabayashi@mp.es.osaka-u.ac.jp

[1] H. Alves, A. S. Molinari, H. Xie, and A. F. Morpurgo, Nature Mater. **7**, 574 (2008).
[2] V. A. Dediu, L. E. Hueso, I. Bergenti, and C. Taliani, Nature Mater. **8**, 707 (2009).
[3] A. Tsumura, H. Koezuka, and T. Ando, Appl. Phys. Lett. **49**, 1210 (1986).
[4] T. Mori *et al.*, Bull. Chem. Soc. Jpn. **57**, 627 (1984).
[5] J. Takeya *et al.*, Appl. Phys. Lett. **90**, 102120 (2007).
[6] V. Podzorov, E. Menard, A. Borissov, V. Kiryukhin, J. A. Rogers, and M. E. Gershenson, Phys. Rev. Lett. **93**, 086602 (2004).
[7] RefCode QQQCIG01, Cambridge Crystallographic Data Centre.
[8] T. Minato, H. Aoki, H. Fukidome, T. Wagner, and K. Itaya, Appl. Phys. Lett. **95**, 093302 (2009).
[9] E. Menard, A. Marchenko, V. Podzorov, M. E. Gershenson, D. Fichou, and J. A. Rogers, Adv. Mater. **18**, 1552 (2006).
[10] S. R. Andrews and R. A. Cowley, J. Phys. C **18**, 6427 (1985).
[11] E. Vlieg, J. F. van der Veen, S. J. Gurman, C. Norris, and J. E. Macdonald, Surf. Sci. **210**, 301 (1989).
[12] Y. Yacoby, M. Sowwan, E. Stern, J. O. Cross, D. Brewe, R. Pindak, J. Pitney, E. M. Dufresne, and R. Clarke, Nature Mater. **1**, 99 (2002).
[13] M. Sowwan, Y. Yacoby, J. Pitney, R. MacHarrie, M. Hong, J. Cross, D. A. Walko, R. Clarke, R. Pindak, and E. A. Stern, Phys. Rev. B **66**, 205311 (2002).
[14] P. R. Willmott, C. M. Schlepuetz, B. D. Patterson, R. Herger, M. Lange, D. Meister, D. Maden, C. Broennimann, E. F. Eikenberry, G. Huelsen, and A. Al-Adwan, Appl. Surf. Sci. **247**, 188 (2005).
[15] P. R. Willmott, S. A. Pauli, R. Herger, C. M. Schlepütz, D. Martoccia, B. D. Patterson, B. Delley, R. Clarke, D. Kumah, C. Cionca, and Y. Yacoby, Phys. Rev. Lett. **99**, 155502 (2007).
[16] Na Sai, Murilo L. Tiago, James R. Chelikowsky, and Fernando A. Reboredo, Phys. Rev. B **77**, 161306(R) (2008).
[17] P. Giannozzi *et al.*, J. Phys. Condens. Matter **21**, 395502 (2009).